The Journal of Chemical Physics

RESEARCH ARTICLE | DECEMBER 22 2023

Fingerprints of hydrogen bonding in the terahertz dynamics of ethanol and water: An inelastic x-ray scattering study

A. De Francesco ; F. Formisano ; L. Scaccia ; E. Guarini ; U. Bafile ; M. A. González ; A. Alatas ; S. T. Lynch ; A. Cunsolo

J. Chem. Phys. 159, 244501 (2023)
https://doi.org/10.1063/5.0180961

The Journal of Chemical Physics ARTICLE pubs.aip.org/aip/jcp

Fingerprints of hydrogen bonding in the terahertz dynamics of ethanol and water: An inelastic x-ray scattering study

Cite as: J. Chem. Phys. 159, 244501 (2023); doi: 10.1063/5.0180961
Submitted: 13 October 2023 • Accepted: 29 November 2023 •
Published Online: 22 December 2023

A. De Francesco,[1,a)] F. Formisano,[1] L. Scaccia,[2] E. Guarini,[3] U. Bafile,[4] M. A. González,[5] A. Alatas,[6] S. T. Lynch,[7] and A. Cunsolo[7]

AFFILIATIONS

[1] CNR-IOM and INSIDE@ILL c/o Operative Group in Grenoble (OGG), F-38042 and Institut Laue Langevin, F-38042 Grenoble, France
[2] Dipartimento di Economia e Diritto, Università di Macerata, via Crescimbeni 20, 62100 Macerata, Italy
[3] Dipartimento di Fisica e Astronomia, Università di Firenze, via G. Sansone 1, I-50019 Sesto Fiorentino, Italy
[4] Consiglio Nazionale delle Ricerche, Istituto di Fisica Applicata "Nello Carrara", via Madonna del Piano 10, I-50019 Sesto Fiorentino, Italy
[5] Institut Laue Langevin, 72 Avenue des Martyrs, F-38042 Grenoble, France
[6] Advanced Photon Source, Argonne National Laboratory, Argonne, Illinois 60439, USA
[7] Department of Physics, University of Wisconsin—Madison, 1150 University Avenue, Madison, Wisconsin 53706, USA

[a)] **Author to whom correspondence should be addressed:** defrance@ill.fr

ABSTRACT

We used inelastic x-ray scattering methods to measure the terahertz spectrum of density fluctuations of ethanol in both liquid and solid phases. The results of a Bayesian inference-based lineshape analysis with a multiple excitation model and the comparison with a previous similar analysis on water indicate that the different structures induced by hydrogen bonds in ethanol and water have a profound influence on the respective dynamic responses, the latter being characterized by longer living and better resolved high-frequency acoustic excitations. In addition, we compare these findings with those obtained with an alternative approach based on the exponential expansion theory and ensuring sum rules fulfillment, demonstrating that the model's choice directly impacts the number of spectral modes detected.

I. INTRODUCTION

Although studies of acoustic propagation in liquid and crystalline media are well documented in the literature, our knowledge of this subject remains qualitative in many aspects. For instance, albeit well-known that, with decreasing wavelengths, disorder and local anisotropy gradually dominate over structural relaxation and diffusion,[1] the link between this crossover and the nature of molecular bonding mostly remains an interpretative challenge. To gain insight into this topic, comparing terahertz propagation in systems with bonding networks of different connectivity and topologies seems especially meaningful. Due to their dissimilar hydrogen bond (HB) properties, water and alcohols appear ideally suited for a comparative study. Indeed, water is often considered an ideal HB system in which two hydrogen atoms and two lone pairs can enable a single molecule to form as many as four hydrogen bonds. In other words, water possesses just the required numbers of hydrogen atoms and lone pairs to have all of them engaged in hydrogen bonding, forming a strongly interconnected tetrahedral arrangement. On the other hand, hydrogen bonding in ethanol is limited by the ability of the molecule to donate only one HB while accepting two, which prevents the formation of a three-dimensional bond network. Furthermore, alcohol molecules are, by definition, amphiphilic, as they contain both non-polar alkyl hydrophobic and polar hydroxyl

hydrophilic parts. The circumstance that hydroxyl groups can experience hydrophobic solvation further increases the complexity of the HB dynamics in alcohols.

Since the mid-1970s, the influence of hydrogen bonding on the dynamics of water has been the focus of intensive experimental[2,3] and computational[4–7] work. This investigative effort supports the conclusion that viscoelastic behavior over picosecond timescales and nanometer distances occurs and primarily arises from fast HB readjustments.[8] A likely manifestation of this high-frequency viscoelasticity is the emergence of an additional low-frequency peak arising from acoustic shear wave propagation.

Similar experimental studies on alcohols are instead more sporadic; among the few examples is a combined inelastic neutron scattering and *ab initio* molecular dynamics study on methanol, evidencing a viscoelastic behavior qualitatively similar to that of water.[9,10] However, previous measurements of another alcohol (ethanol) outlined, not without some controversy,[11–14] a less complex dynamic behavior with no clear evidence of transverse dynamics.[15] Given the importance of establishing direct connections between the collective dynamics and the nature of the HB-induced structures in these and other liquid systems, we used Inelastic X-Ray Scattering (IXS) to jointly investigate the dynamics of ethanol in both liquid and solid phases and compare these measurements with previous ones we obtained in water.[16]

The scarcity of IXS studies on ethanol is, to some extent, surprising, as this sample presents various intriguing aspects, including the presence of polymorphic phases upon quenching, namely a fully disordered, canonical glass, an orientationally disordered crystal, and a fully ordered (monoclinic) one. Concerning the terahertz collective dynamics, a difference between water and ethanol emerging from available investigations is the ability to support shear or transverse terahertz acoustic propagation. Several works on water documented the presence of both a transverse and a longitudinal sound mode in the spectrum of density fluctuations $S(Q,E)$,[7,17–19] where Q and E are the energy transfer, respectively. Conversely, the only available IXS study on ethanol[15] indicated, despite the controversy mentioned,[11] that no fingerprint of shear dynamics exists in the spectrum in either ordered or disordered phases. Furthermore, the same work highlighted close resemblances in the dynamics of the two solid species (glassy and crystalline) of ethanol, somehow at odds with the well-known differences in the thermal properties of the two phases. The likely reason for this apparent inconsistency is that heat transport anomalies of glassy ethanol are primarily associated with transverse acoustic modes only, whose observation, in Ref. 15, was hampered by the relatively wide resolution profile.

To shed some light on the topics discussed earlier, we investigate the Q dependence of $S(Q,E)$ of ethanol, measured in the liquid phase just above the melting temperature T = 158.9 K and in the fully ordered (monoclinic) crystal phase at the beamline Sector 3 of the Advanced Photon Source (APS) at Argonne National Laboratory.[20,21] Preparing the crystal phase of ethanol requires quenching at 97 K (at a rate of no less than 6 K/min) and subsequent annealing at about 130 K for at least a half hour.[22] Analyzing measured lineshapes with alternative models enables us to elucidate distinctive and shared aspects of the two samples. A detailed analysis of the IXS spectrum of disordered systems suffers from significant uncertainties, mainly arising from the loosely discernible spectral features under scrutiny. These limitations make the interpretation of the scattering signal heavily dependent on statistical accuracy and energy resolution. To make the situation even more puzzling, the physical insight sought from experimental data is becoming increasingly sophisticated and often at the limit of current spectrometer capabilities. Properly addressing these difficulties requires evidence-based lineshape analyses beyond the capability of traditional χ^2 fitting approaches.

Fortunately, Bayesian inference meets these requirements, and it has recently proved to be an effective modeling tool.[23–27] Along this line, the Bayesian method employed here enables an unbiased analysis of the lineshape from water and ethanol and the recognition of the spectral modes that contribute to the spectra. These assets permitted us to interpret the spectrum of density fluctuations more reliably and to unveil the different roles played by HB interactions in water and ethanol. Bayesian inference has the undoubted merit of addressing limitations in the prior knowledge of the problem under study, providing immunity against the risk of data over-interpretation and unnecessary model complexity. However, the widely adopted lineshape models, inclusive of one or more Damped Harmonic Oscillator (DHO) profiles, while often adequate to approximate the overall spectral shape, have diverging low-order spectral moments. To assess any model dependence of the achieved results, we compared the results of the Bayesian analysis with those of Exponential Expansion Theory (EET) modeling, which incorporates the fulfillment of a typically higher number of sum rules.

II. THE LINESHAPE MODELING

A realistic model of the measured lineshape should also account for the various experimental factors affecting the spectral measurement, including the environmental background and the instrumental resolution broadening. In practice, the model ultimately fitting each scattering profile has the following form:

$$I(Q,E) = R(E) \otimes S(Q,E) + B(E), \tag{1}$$

where $\otimes$ represents the convolution operator, $R(E)$ is the experimental energy resolution function of the instrument, and $B(E) = b_0 + b_1 E$ is a linear term accounting both for the spectral background and the electronic noise of the detectors.

A. The Bayesian analysis

We performed a Bayesian inference-based analysis of the measured spectra, whose details were discussed in previous works[23,25,28] and which exploits a Markov Chain Monte Carlo (MCMC)[29,30] algorithm integrated by a Reversible Jump[31] (RJ) routine.[23] Measured lineshapes were approximated with a model including several DHO excitation profiles,[32] whose numbers, instead of being guessed *a priori*, were estimated from the data. When dealing with a solid sample, the inelastic excitations were complemented by a $\delta(E)$ profile—with $\delta(E)$ being the Dirac delta function of the energy—accounting for the elastic signal. For the liquid phase, a Lorentzian function,

$$L(E) = \frac{1}{\pi} \frac{A_0(Q) z_0(Q)}{E^2 + z_0^2(Q)},$$

was used instead. This term contains the two Q-dependent parameters A_0 and z_0, representing its amplitude and half-width, respectively.

In summary, when modeling the spectrum of density fluctuations in the solid sample, we used the following form:

$$S(Q,E) = A_e(E)\delta(E) + [n(E)+1]\frac{E}{k_BT}\left\{\sum_{j=1}^{k} A_j \mathrm{DHO}_j(Q,E)\right\}, \quad (2)$$

where A_e represents the area of the elastic peak. For liquid ethanol, we used instead

$$S(Q,E) = [n(E)+1]\frac{E}{k_BT}\left\{L(E) + \sum_{j=1}^{k} A_j \mathrm{DHO}_j(Q,E)\right\}. \quad (3)$$

In both cases, each term in the sum accounts for an inelastic excitation in the spectrum, with

$$\mathrm{DHO}_j(Q,E) = \frac{2}{\pi}\frac{\Omega_j^2(Q)\Gamma_j(Q)}{(E^2-\Omega_j^2(Q))^2 + 4[E\Gamma_j(Q)]^2}, \quad (4)$$

where Ω_j, Γ_j, and A_j are the undamped frequency, the damping coefficient, and the area, respectively.

The energy-dependent term $[n(E)+1]E/k_BT$ guarantees the compliance of the spectrum with the detailed balance principle, with k_B being the Boltzmann constant, T the sample temperature, and $n(E) = (\exp(E/k_BT)-1)^{-1}$ the Bose statistics factor. In the following, we drop the explicit mention of the Q dependence of all spectral parameters. Noticeably, as remarked, the number, k, of DHO profiles included in the model is here a free parameter whose optimal value is to be determined by the Bayesian inference algorithm conditional on the measurement outcome. As for all other model parameters, the background parameters b_0 and b_1 have been estimated by the MCMC-RJ algorithm conditional on the experimental data for each single spectrum. As an output, this approach provides the posterior distributions for each single model parameter and the posterior distribution $P(k|y)$ of the number of inelastic modes given the measured data y. The Bayesian algorithm selects the value $k = 2$ for the most reliable model, with an associated probability between 0.78 and 0.99. However, despite these large values, the posterior distributions for the high-frequency mode parameters Ω_2 and Γ_2 appear to have a broad shape at specific Q values, which reflects the problematic identification of this excitation in the spectra.

B. The exponential expansion theory lineshape model

The exponential expansion theory[33–35] predicts that any autocorrelation function can be expressed as a series of exponential terms (called *modes*). Therefore, at each Q value, the van Hove intermediate scattering function $F(Q,t)$[36] can be represented, at $t \geq 0$, by

$$F(Q,t) = F(Q,0)\sum_{j=1}^{\infty} I_j \exp(z_j t). \quad (5)$$

In Eq. (5), relaxation processes are accounted for by exponentially decaying terms with real I_j and z_j (with $z_j < 0$), while exponentially damped oscillatory components of the correlation are represented in the series by "complex pairs," i.e., by $I_j \exp(z_j t) + I_j^* \exp(z_j^* t)$, with complex I_j and z_j and $\mathrm{Re}z_j < 0$. Note that complex modes appear in conjugate pairs because the correlation function corresponding to a symmetric (i.e., not asymmetrized according to detailed balance) spectrum is real-valued. In Eq. (5), I_j and z_j are functions of Q, although we omitted this dependence in the above-mentioned notation.

As a consequence of the exponential functional form of the time autocorrelation function, the (normalized) frequency spectrum reads

$$\frac{S(Q,E)}{S(Q)} = \sum_{j=1}^{\infty} L_j(E) = \sum_{j=1}^{\infty} \frac{I_j}{\pi}\left[\frac{(-z_j)}{E^2+z_j^2}\right], \quad (6)$$

where $L_j(E)$ is a "generalized" Lorentzian line. If I_j and z_j are real, then $L_j(E)$ is a genuine Lorentzian centered at $E = 0$ and characterized by a half width at half maximum equal to $-z_j$. If I_j and z_j are complex, then the corresponding mode and its complex conjugate add up to give a pair of distorted Lorentzians centered at the nonzero energies $\pm\mathrm{Im}z_j$ [see Eq. (4) of Ref. 37 for details].

The EET has enabled very accurate descriptions of various correlation functions and spectra of interest in studies of the self[37,38] and the collective dynamics[39,40] of fluids. Details on its application can be found in Refs. 37–39. Essentially, the analysis consists of performing a fitting procedure to determine the parameters z_j and I_j of a small number p of modes, which the sum in Eq. (5) in practice reduces to. Here, we note that $p-1$ constraints are imposed on the amplitudes I_j to enforce the vanishing of the first few odd-time derivatives of $F(Q,t)$ at $t = 0$, or, equivalently, the finiteness of the first few even frequency moments of the spectra.[39]

For liquid ethanol spectra at 160 K, a single-excitation model with one additional decay (real) mode accurately describes the low-Q spectral shape (see Fig. 3). The imposed physical constraints at small Q ensure the convergence of the second spectral moment. At $Q = 13.91$ nm^{-1} and at $Q \geq 23.77$ nm^{-1}, the ethanol spectra are best fitted with an EET profile containing three excitations (see discussion), at variance with the Bayesian analysis results, supporting the presence of two inelastic doublets only. The best-fit procedure with the EET model could be performed by enforcing the convergence of the even spectral moments up to the tenth order. In the supplementary material (Fig. S3), we compare the optimal model lineshapes of the $Q = 13.91$ nm^{-1} spectrum obtained with the three-excitation EET model and with the MCMC algorithm in the case where RJ is disabled, k is no longer a free parameter, and the $k = 3$ value is imposed. Not surprisingly, the two lineshapes look very similar, apart from the slightly different relative intensity of the inelastic doublets and the DHO profiles having slightly lower undamped frequencies. The reason for this discrepancy is subtle and ultimately relates to the convergence of the spectral moments incorporated in the EET description.

A comment is worth making concerning the EET fits in the Q range (around the wavevector $Q_p \simeq 17$ nm^{-1}, corresponding to the main peak of the static structure factor in liquid ethanol), where the well-known propagation gap of longitudinal waves takes place, causing the vanishing of their frequency $\mathrm{Im}z_j$. In such a Q region, appropriate EET modeling requires substituting the longitudinal complex pair found at other Q values (i.e., outside the gap) with two real modes. However, in such conditions, the fits become unstable

and do not properly determine the three central lines (one relaxation mode plus the two real modes related to the overdamped longitudinal spectral component). Therefore, at Q = 17.24 and 20.50 nm^{-1}, we assumed a simplified model consisting of one central Lorentzian and two complex pairs, the latter accounting only for the lowest and highest frequency modes detected by the EET approach outside the gap. Notice that, for a meaningful comparison with the parameters Ω_j of the DHO lineshapes, in displaying the EET frequencies, we plot the corresponding quantities $\Omega_j = \sqrt{(\mathrm{Re}z_j)^2 + (\mathrm{Im}z_j)^2}$.

III. DISCUSSION OF RESULTS

A. The liquid phase

Figure 1 compares the IXS spectra of liquid water and ethanol with corresponding fitted model lineshapes and individual low-frequency (green line) and high-frequency (blue line) components, here assigned to transverse and longitudinal acoustic modes, respectively. All these model lineshapes include the detailed balance factor and are resolution-convoluted. The semi-logarithmic plot emphasizes the agreement between raw spectra and fitted lineshapes across the various decades spanned by the intensity profiles. While the water spectra in Fig. 1 have been shown in our previous work,[16] ethanol measurements are discussed here.

Both samples display a spectral shape fairly typical for liquid systems, mainly featuring wide and loosely resolved inelastic shoulders on the side of a dominant central peak. As it appears from the central panel of the left column, the side shoulders make the spectral shape of the sample neatly distinguishable from the resolution profile, also reported after appropriate re-scaling. In the same plot, the algorithm-estimated background is also included for reference; its comparison with the sample spectrum emphasizes that an excellent signal-to-noise ratio was achieved in the measurement, even in the region of spectral tails.

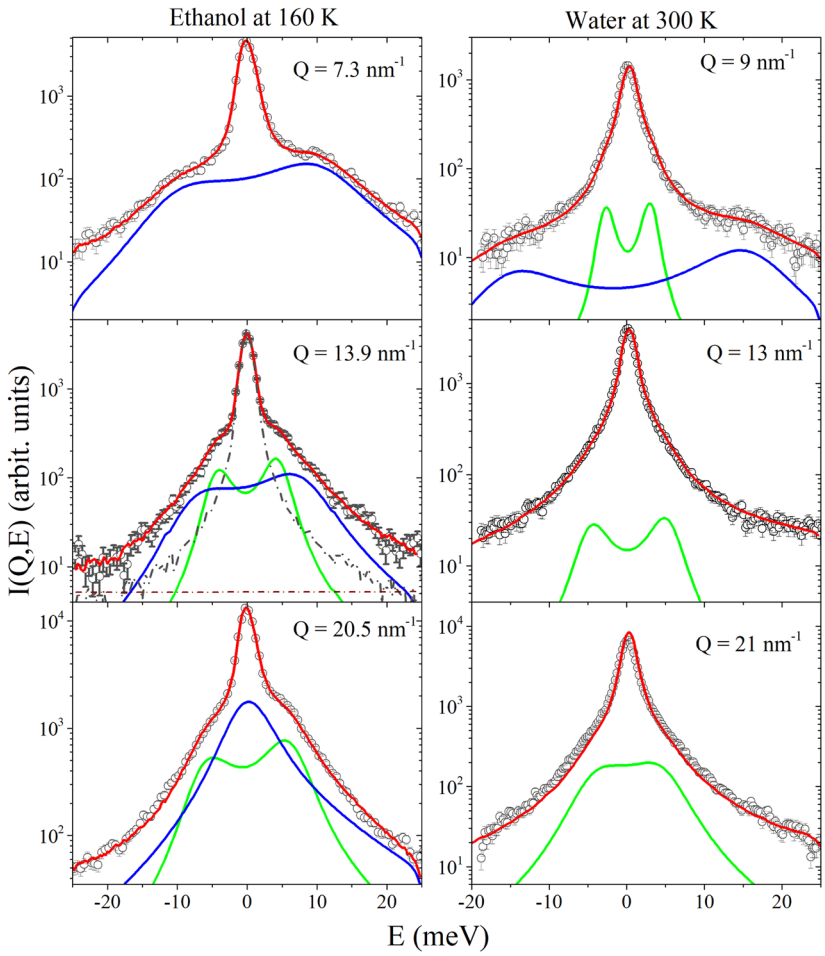

FIG. 1. A few representative IXS spectra (dots), measured on liquid ethanol in this work and on water in our previous work in Ref. 16 at the Q values and temperatures indicated, are compared with their optimal model lineshapes (red line) and their transverse acoustic (green line) and longitudinal acoustic components (blue line). In the middle left panel, the dash–dotted black line indicates the experimental resolution profile, and the wine–dotted line is the estimated linear background. Model lineshapes were obtained with the Bayesian inference method described in the text.

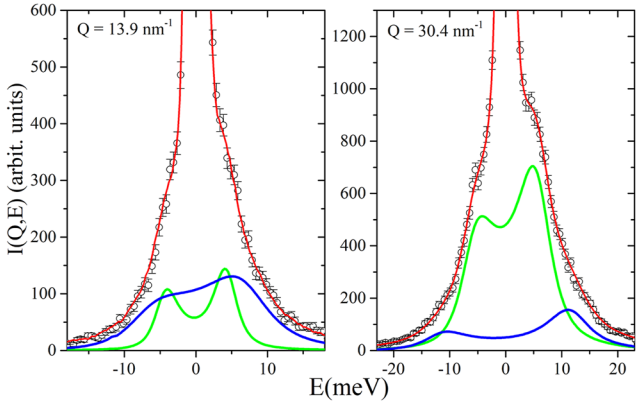

FIG. 2. IXS measured spectra of ethanol at 160 K and at two high Q values are reported on a linear and expanded scale. The lines and symbols are as in Fig. 1.

One can readily notice that, at Q larger than 9 nm^{-1}, water spectra bear no evidence for a longitudinal mode at all, unlike their ethanol counterparts. Partly, the disappearance of the longitudinal acoustic mode owes to the limited energy transfer range spanned by the measurement in water. However, it also stems from the steep Q-increase of the longitudinal damping in liquid water. Conversely, in ethanol spectra, the longitudinal mode always contributes to a sizeable portion of the inelastic signal. In the ethanol spectrum at $Q = 20.5$ nm^{-1}, the longitudinal mode appears as a single featureless quasielastic peak, as is to be expected when Q is in the proximity of Q_p. The longitudinal mode might be visible at Q as large as 30.4 nm^{-1}, as shown in Fig. 2. There, one can find more convincing evidence of the persistence of a double shoulder feature in the spectral profile of ethanol by looking at the spectral shape on a linear scale and in an expanded view. Although the lower frequency mode largely dominates the high Q scattering profile of ethanol, the longitudinal one remains visible well beyond Q_p.

There are sound reasons to ascribe the lower frequency mode to a transverse acoustic excitation. One may object that, although in water, the transverse acoustic nature of the lower frequency inelastic mode is supported by abundant evidence,[7,17,18,41] no comparable evidence supports the onset of transverse acoustic propagation in the terahertz spectrum of the density fluctuations. However, the density of states[42] and coherent neutron scattering[11] measurements did indicate the existence of such a transverse acoustic mode in the dynamic response of ethanol. Furthermore, a similar transverse acoustic excitation was later found in methanol.[9,10] Finally, the dispersion behavior and energy of the low-frequency mode observed here resemble those of the transverse acoustic mode already observed in a broad class of disparate liquids.[43]

The onset and high Q persistence of a double excitation profile have been observed using both approaches discussed in the previous section. As mentioned, when the reduced χ^2 is properly minimized, the EET-based curve fitting exploiting the EET indicates the presence of a third high-frequency mode. It is reasonable to infer that the sum rules compliance, owing to the more rapid decay it induces on spectral wings, enables the EET modeling to spot barely emerging high-frequency spectral features. On the other hand, the limited energy transfer range explored makes the evidence of this third excitation hardly robust enough to draw any conclusion on its phenomenology and dispersive behavior. We only remark a perhaps significant resemblance of this mode with the one we previously observed in methanol,[9,10] which indeed appeared as a weakly dispersing excitation with an energy between 26 and 30 meV, which ascribes to a typical vibration mode in hydrogen bonded liquids. In Fig. 3, a comparison at selected Q values is shown between the fits of the spectral lineshapes obtained using the Bayesian approach and the EET. Although the Bayesian analysis did not find sufficient experimental evidence for a third inelastic mode, the overall agreement between the two analysis methods is quite evident, especially in the characterization of the two acoustic modes.

Until now, we have gained a coherent understanding of the qualitative differences between the spectral responses of ethanol and water, two samples characterized by a hydrogen bond network of different rigidity and topology. To complement the outlined scenario, we add a few general considerations on the IXS spectral density of ethanol measured at temperatures higher than 160 K. At these temperatures, the spectra measured in ethanol can be consistently described by using a single highly damped DHO profile, as briefly discussed in the supplementary material. This finding indicates that, at variance with liquid water, the spectrum of ethanol at moderately low or ambient temperatures does not display direct evidence for a transverse excitation. This trend is likely a consequence of the highly damped nature of collective modes and the consequent difficulty in mutually resolving them in the lineshape.

Finally, we remark that a meaningful indicator of damping effects is the ratio of the damping to the excitation frequency. At $Q = 13.9$ nm^{-1}, the values of this ratio are 0.40 and 0.25 for the transverse and longitudinal excitations, respectively. The corresponding values at $Q = 30.4$ nm^{-1} are 0.58 and 0.45. In general, the relative damping of the transverse mode in ethanol is consistently slightly larger than in its longitudinal counterpart.

B. Exploring the solid phase

So far, we have discussed qualitative aspects of ethanol and water spectra in the liquid phase. A question arises about how the observed behavior changes when the two samples are in the solid phase, where differences in the HB rigidity are arguably more pronounced. Figure 4 addresses this question directly by comparing a selection of IXS spectra measured with the same spectrometer either on polycrystalline ice Ih or in monoclinic crystal ethanol at the respective temperatures of 225 and 50 K and at similar Q values. Again, measurements on ice are those already discussed in our previous work,[16] while their ethanol counterparts were performed in this work. Notice that spectral measurements on ethanol cover a broader Q range due to the need to fully capture the tails of the broad inelastic shoulders. From a qualitative inspection of the plots, a few general trends readily emerge: (1) Despite the much higher temperature, ice spectra display sharper inelastic peaks, as expected for a highly ordered and "rigid" system whose sound velocity is significantly higher than in ethanol. (2) The longitudinal phonon of ice, albeit dominant at low Q, rapidly loses visibility as Q increases, disappear-

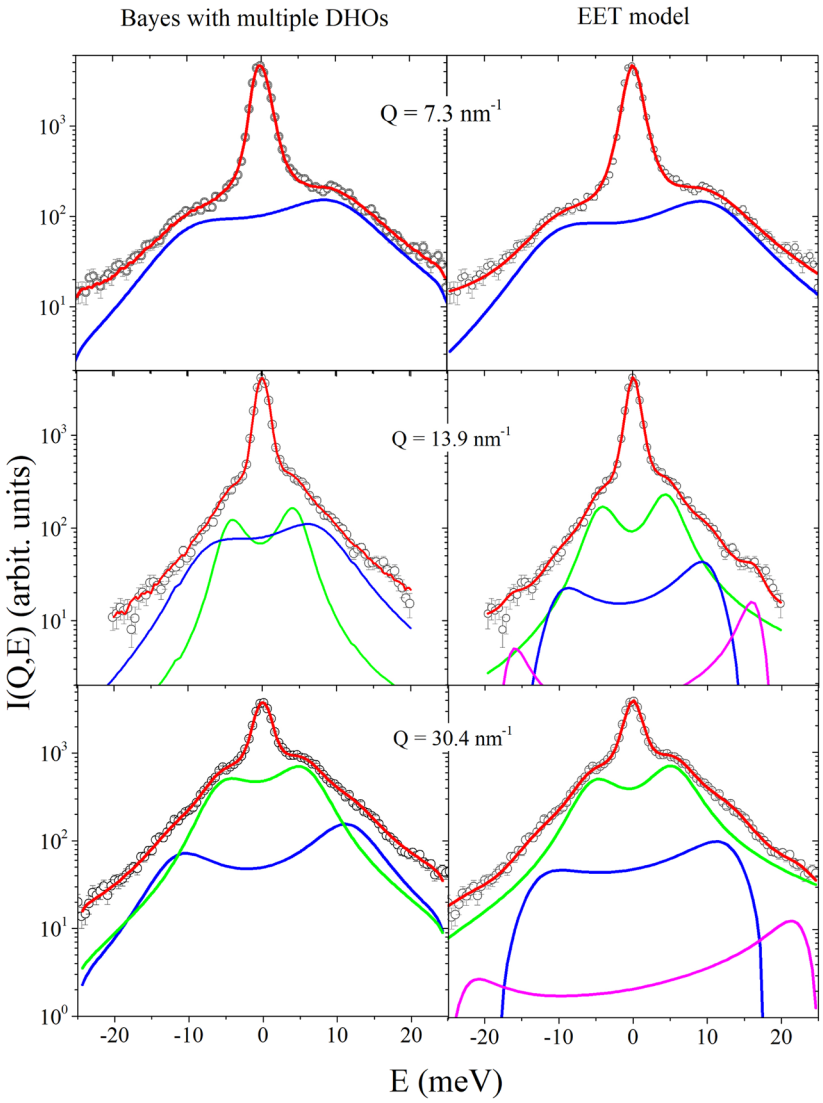

FIG. 3. IXS spectra measured at representative Q's and T = 160 K discussed in this work (open circles) compared with corresponding fitted lineshapes (red lines through data) along with their inelastic model components (see text): the low-frequency transverse mode (green line) and the longitudinal acoustic mode (blue line). Left column: best fit as determined by the Bayesian analysis exploiting an MCMC-RJ[23] algorithm. Right column: best fit as obtained by the EET theory. The pink line corresponds to the high-frequency mode revealed by the EET. Error bars are estimated as the square root of the scattering intensity counts.

ing entirely at $Q = 21$ nm^{-1}. This trend can be readily appreciated by following the dashed arrow marking the Stokes peak position. (3) At even higher Q, no measurement is available for ice, while the ethanol spectra exhibit a longitudinal peak of sizable intensity, as suggested by the two optimal DHO model profiles, also included in the plot for reference.

C. The dispersion curves

Our last considerations focus on a more quantitative aspect, such as the dispersion curve of the two acoustic branches of ethanol and water as derived in the liquid and solid phases and how these relate to existing literature data. Figure 5 compares these dispersion curves with literature results[42,44] for the density of states (DoS) measured in the crystalline phases of ethanol and water. The same plot also includes the IXS measurement on the crystal monoclinic phase by Matic and collaborators,[15] who did not observe distinct transverse modes, as mentioned in the introductory section. For liquid ethanol, the EET results are also shown in Fig. 5. A good agreement between the EET and Bayesian determinations of the transverse and longitudinal branches can be readily appreciated. However, as discussed in Sec. II B, EET fails to identify the longitudinal undamped

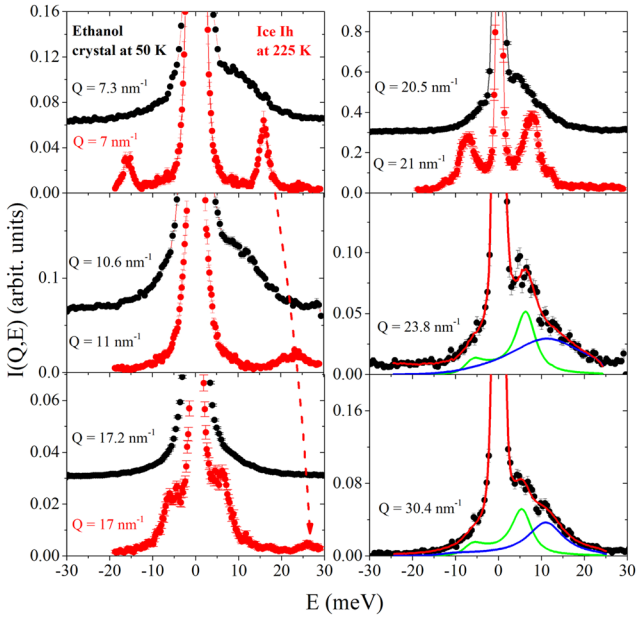

FIG. 4. IXS spectra measured at representative Q's for crystalline ethanol and pure ice. Spectral shapes are normalized to their maximum intensity, attained at the elastic scattering position $E = 0$, and ethanol spectra are vertically offset for clarity. At the largest Q values, only the spectra for ethanol are available and compared with corresponding fitted lineshapes (red lines through data). In addition, the inelastic DHO model components are included for reference: the low-frequency transverse mode (green line) and the longitudinal acoustic mode (blue line). The dashed arrow on the left plot marks the position of the Stokes peak corresponding to the longitudinal acoustic mode in pure ice.

frequency at the two Q values close to Q_p, which explains why two green points are missing in the figure. Moreover, the position of the highest frequency mode of the EET spectrum is also plotted for reference. Although we currently do not have a clear understanding of the physical origin of this additional dispersion branch, we already noticed its resemblance to a similar high-frequency mode previously found in methanol and ascribed to hydrogen bonding.[10]

Concerning ice, one can readily appreciate the excellent agreement between the energy position of the DoS peaks and the maxima of the dispersion curves, where, due to the vanishing Q-derivative of Ω, there is indeed a pile-up of phonon states, commonly referred to as Van Hove singularity.[45] The dashed horizontal arrows in the plot show a correspondence between dispersion curve maxima and poles in the DoS. Data include both the longitudinal acoustic (higher energy) and transverse acoustic (lower frequency) dispersion curves, as measured in water in previous IXS works.[16,17]

Although a similar correspondence also exists in ethanol data, the two samples appear to drastically differ in at least two related aspects, as follows:

(1) In ethanol, the distance between the DoS maxima corresponding to the longitudinal acoustic and the transverse acoustic dispersion branches is much smaller than in ice.

(2) The corresponding DoS features of ethanol are visibly broader, thus preventing a proper resolution of the longitudinal acoustic and transverse acoustic contributions, the latter mostly appearing as a side shoulder. Both features seem to be manifestations of the higher rigidity of the HB network in ice compared to the HB-induced structures in ethanol. More specifically, they appear to reflect this rigidity in the lifetime of density fluctuation, which in ice is longer and sharper.

Finally, in Fig. 6, for completeness, we report the dispersion curves of the acoustic longitudinal and transverse modes measured in this work for the crystalline phase compared with the dispersion of the longitudinal acoustic mode previously observed by Matic *et al.*[15] The comparison highlights the consistency between independent measurements taken almost two decades apart. Moreover, the excellent agreement between the longitudinal dispersion measured in liquid and solid ethanol can be readily appreciated. The absence of a transverse branch in the measurement by Matic and collaborators in the solid phase may appear more baffling, given the expected higher ability of a solid to support shear acoustic propagation. The most likely explanation is the inherent limitation in both count statistics and resolution combined with the tendency of the line shape to preserve its liquid-like nature, i.e., its significant damping and low propagation speed, well below the melting, as extensively discussed in this work.

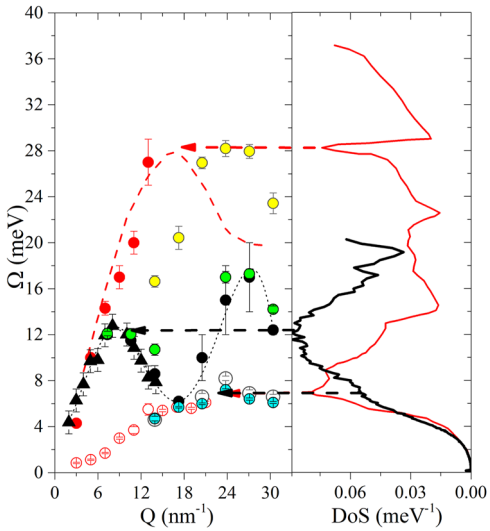

FIG. 5. Left panel. The following dispersion curves are shown: the longitudinal acoustic mode (black triangles) in monoclinic crystal ethanol as measured by Matic *et al.*[15] with the x-ray synchrotron beamline ID 16 at ESRF (Grenoble, France); the transverse acoustic (TA) (empty black dots) and longitudinal acoustic (LA) modes (full black dots) of liquid ethanol measured in the present work by the Sector 3 beamline at APS (Argonne, USA) in a higher Q momentum transfer interval; the TA (empty red dots) and LA (full red dots) modes in liquid water as in Ref. 16; the LA (dashed red line) determined by Pontecorvo *et al.*[17] Finally with full cyan, green and yellow dots the three excitation frequencies as determined by the EET are shown. Right panel. Density of states in monoclinic crystal ethanol[42] (black) and in I_c ice[44] (red).

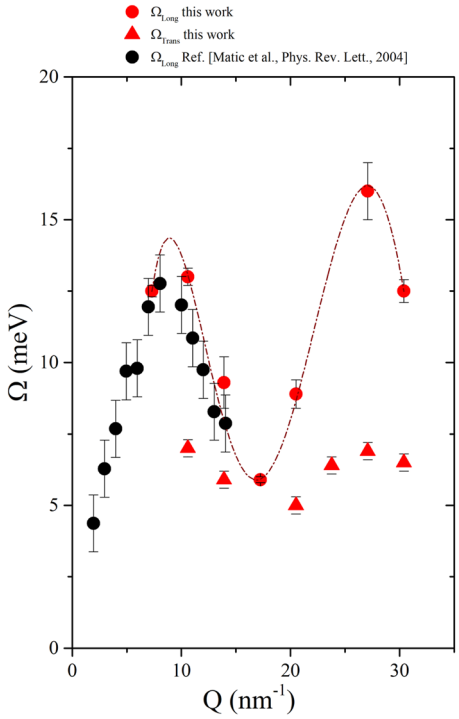

FIG. 6. Dispersion curves of the longitudinal acoustic mode in monoclinic crystal ethanol as measured by Matic *et al.*[15] with the x-ray synchrotron beamline ID 16 at ESRF (Grenoble, France) (black dots) and of the transverse acoustic (TA) (red triangles) and longitudinal acoustic (LA) modes (red dots) of crystalline (monoclinic) ethanol measured in the present work by the Sector 3 beamline at APS (Argonne, USA) in a higher Q momentum transfer interval and at $T = 50$ K. The red dot line is a guide for the eye.

IV. CONCLUSION

In conclusion, we have measured the IXS lineshapes of ethanol in both its crystalline (monoclinic) and liquid phases. The IXS spectra were analyzed with two parallel approaches, either based on a Bayesian inference method on a model having an adjustable number of simple damped harmonic oscillator profiles or with an exponential expansion theory model on which a few sum rules were imposed. In either case, we found solid evidence for a double-mode structure arising from longitudinal and transverse acoustic propagation. The comparison with recent measurements on water suggests that due to the weaker hydrogen bonding, longitudinal and transverse acoustic modes in ethanol are significantly broader and sit at closer energy than in water, with these differences becoming especially pronounced in the crystal phase. This substantial acoustic damping, combined with energy resolution limitations, makes the proper resolution of the two acoustic modes challenging and, in the past, has likely prevented the appropriate observation of a transverse excitation in the ethanol spectrum. Finally, measured scattering profiles show evidence for an additional high-energy spectral mode already observed in methanol, whose physical origin remains obscure, although it has been associated in the past with the presence of H-bonding. Properly characterizing this higher frequency feature prompts further measurements or simulation efforts covering a broader energy range, possibly including other systems having hydrogen bond networks of different topologies and site connectivity.

In summary, the main result of the present work is the observed similarity of the dynamics response of ethanol in the liquid and crystalline phases. As surprising as it is, this observation is consistent with previous literature, which is here complemented by the comparison with a more interconnected system, such as water. We are urged to associate the observed differences to the quite distinctive hydrogen bond properties of ethanol and water.

It is finally important to point out the inherent challenges associated with a clear-cut distinction between the diffusive or propagating nature of collective modes in complex systems. This difficulty also arises from the low energy and large damping of these modes, which can lead to their partial overlap. Further challenges stem from the resolution broadening, the limited count statistics, and the narrow energy range covered. To cope with all these issues, it becomes essential to resort to modeling approaches that are physically grounded and inherently unbiased. In this spirit, the present work discusses the first attempt to combine the rigor and generality of EET with the rooting into evidence of the Bayesian method. A natural extension of the presented analysis can be accomplished by integrating these two approaches into a single modeling framework.

SUPPLEMENTARY MATERIAL

We included a few additional figures and related comments in the supplementary material. The first figure shows a comparison of inelastic x-ray scattering spectra collected at three different temperatures: just above the melting point and at two higher temperatures. The second figure shows that ethanol spectra collected at temperatures higher than those probed in this work have an essentially featureless shape, simply appearing as a visibly broadened single peak. Finally, in the third figure, we show that EET and the Bayesian analyses provide identical results once the reversible jump option is switched off and a three-mode model is imposed on the data.

ACKNOWLEDGMENTS

This research used resources from the Advanced Photon Source, a U.S. Department of Energy (DOE) Office of Science user facility operated for the DOE Office of Science by Argonne National Laboratory under Contract No. DE-AC02-06CH11357.

AUTHOR DECLARATIONS

Conflict of Interest

The authors have no conflicts to disclose.

Author Contributions

A.C. designed the research; A.C. and A.A. executed the IXS measurements; A.D.F. and L.S. performed the Bayesian analysis; E.G. performed the EET analysis; A.C., A.D.F., L.S., F.F., E.G., U.B.,

M.A.G., and S.T.L. wrote the manuscript, which was then critically revised, commented on, and approved by all the authors. All the authors have read and agreed to the published version of the manuscript.

A. De Francesco: Data curation (lead); Formal analysis (lead); Methodology (lead); Software (lead); Supervision (equal); Validation (equal); Writing – original draft (equal); Writing – review & editing (lead). **F. Formisano**: Investigation (equal); Validation (equal); Writing – review & editing (equal). **L. Scaccia**: Software (equal); Validation (equal); Writing – original draft (equal); Writing – review & editing (equal). **E. Guarini**: Formal analysis (equal); Methodology (equal); Software (equal); Validation (equal); Writing – original draft (equal); Writing – review & editing (equal). **U. Bafile**: Formal analysis (equal); Methodology (equal); Software (equal); Validation (equal); Writing – original draft (equal); Writing – review & editing (equal). **M. A. González**: Validation (equal); Writing – review & editing (equal). **A. Alatas**: Data curation (equal). **S. T. Lynch**: Validation (equal); Writing – review & editing (equal). **A. Cunsolo**: Conceptualization (lead); Data curation (lead); Formal analysis (equal); Investigation (lead); Supervision (lead); Validation (lead); Writing – original draft (lead); Writing – review & editing (lead).

DATA AVAILABILITY

The data that support the findings of this study are available from the corresponding author upon reasonable request.

REFERENCES

[1] V. M. Giordano and G. Monaco, "Fingerprints of order and disorder on the high-frequency dynamics of liquids," Proc. Natl. Acad. Sci. U. S. A. **107**, 21985–21989 (2010).

[2] J. Teixeira, M. Bellissent-Funel, S. Chen, and B. Dorner, "Observation of new short-wavelength collective excitations in heavy water by coherent inelastic neutron scattering," Phys. Rev. Lett. **54**, 2681 (1985).

[3] A. Cunsolo and M. Nardone, "Velocity dispersion and viscous relaxation in supercooled water," J. Chem. Phys. **105**, 3911–3917 (1996).

[4] A. Rahman and F. H. Stillinger, "Molecular dynamics study of liquid water," J. Chem. Phys. **55**, 3336–3359 (1971).

[5] R. Impey, P. Madden, and I. McDonald, "Spectroscopic and transport properties of water: Model calculations and the interpretation of experimental results," Mol. Phys. **46**, 513–539 (1982).

[6] F. Sciortino and S. Sastry, "Sound propagation in liquid water: The puzzle continues," J. Chem. Phys. **100**, 3881–3893 (1994).

[7] M. Sampoli, G. Ruocco, and F. Sette, "Mixing of longitudinal and transverse dynamics in liquid water," Phys. Rev. Lett. **79**, 1678 (1997).

[8] A. Cunsolo, G. Ruocco, F. Sette, C. Masciovecchio, A. Mermet, G. Monaco, M. Sampoli, and R. Verbeni, "Experimental determination of the structural relaxation in liquid water," Phys. Rev. Lett. **82**, 775 (1999).

[9] S. Bellissima, S. De Panfilis, U. Bafile, A. Cunsolo, M. A. Gonzalez, E. Guarini, and F. Formisano, "The hydrogen-bond collective dynamics in liquid methanol," Sci. Rep. **6**, 39533 (2016).

[10] S. Bellissima, M. A. Gonzalez, U. Bafile, A. Cunsolo, F. Formisano, S. De Panfilis, and E. Guarini, "Switching off hydrogen-bond-driven excitation modes in liquid methanol," Sci. Rep. **7**, 10057 (2017).

[11] F. Bermejo, R. Fernandez-Perea, and A. Krivchikov, "Comment on 'Crystal-like nature of acoustic excitations in glassy ethanol,'" Phys. Rev. Lett. **98**, 229601 (2007).

[12] A. Matic, C. Masciovecchio, D. Engberg, G. Monaco, and L. Börjesson, "Reply to comment on: Crystal-like nature of acoustic excitations in glassy ethanol," Phys. Rev. Lett. **98**, 229602 (2007).

[13] C. Talon, M. A. Ramos, and S. Vieira, "Low-temperature specific heat and glassy dynamics of a polymorphic molecular solid," Phys. Rev. B **58**, 745 (1998).

[14] A. I. Krivchikov, A. N. Yushchenko, V. G. Manzhelii, O. A. Korolyuk, F. J. Bermejo, R. Fernández-Perea, C. Cabrillo, and M. A. González, "Scattering of acoustic phonons in disordered matter: A quantitative evaluation of the effects of positional versus orientational disorder," Phys. Rev. B **74**, 060201 (2006).

[15] A. Matic, C. Masciovecchio, D. Engberg, G. Monaco, L. Börjesson, S. Santucci, and R. Verbeni, "Crystal-like nature of acoustic excitations in glassy ethanol," Phys. Rev. Lett. **93**, 145502 (2004).

[16] A. De Francesco, L. Scaccia, F. Formisano, E. Guarini, U. Bafile, M. Maccarini, A. Alatas, Y. Q. Cai, and A. Cunsolo, "The terahertz dynamics of an aqueous nanoparticle suspension: An inelastic x-ray scattering study," Nanomaterials **10**, 860 (2020).

[17] E. Pontecorvo, M. Krisch, A. Cunsolo, G. Monaco, A. Mermet, R. Verbeni, F. Sette, and G. Ruocco, "High-frequency longitudinal and transverse dynamics in water," Phys. Rev. E **71**, 011501 (2005).

[18] A. Cunsolo, C. Kodituwakku, F. Bencivenga, M. Frontzek, B. Leu, and A. Said, "Transverse dynamics of water across the melting point: A parallel neutron and x-ray inelastic scattering study," Phys. Rev. B **85**, 174305 (2012).

[19] A. Cimatoribus, S. Saccani, F. Bencivenga, A. Gessini, M. Izzo, and C. Masciovecchio, "The mixed longitudinal–transverse nature of collective modes in water," New J. Phys. **12**, 053008 (2010).

[20] T. S. Toellner, A. Alatas, and A. H. Said, "Six-reflection meV-monochromator for synchrotron radiation," J. Synchrotron Rad. **18**, 605–1611 (2011).

[21] A. Alatas, B. Leu, J. Zhao, H. Yavaş, T. Toellner, and E. Alp, "Improved focusing capability for inelastic x-ray spectrometer at 3-ID of the APS: A combination of toroidal and Kirkpatrick-Baez (KB) mirrors," Nucl. Instrum. Methods Phys. Res., Sect. A **649**, 166–168 (2011), National Synchrotron Radiation Instrumentation conference in 2010.

[22] A. Srinivasan, F. J. Bermejo, A. de Andrés, J. Dawidowski, J. Zúñiga, and A. Criado, "Evidence for a supercooled plastic-crystal phase in solid ethanol," Phys. Rev. B **53**, 8172–8175 (1996).

[23] A. De Francesco, E. Guarini, U. Bafile, F. Formisano, and L. Scaccia, "Bayesian approach to the analysis of neutron Brillouin scattering data on liquid metals," Phys. Rev. E **94**, 023305 (2016).

[24] A. De Francesco, U. Bafile, A. Cunsolo, L. Scaccia, and E. Guarini, "Searching for a second excitation in the inelastic neutron scattering spectrum of a liquid metal: A Bayesian analysis," Sci. Rep. **11**, 13974 (2021).

[25] A. De Francesco, A. Cunsolo, and L. Scaccia, "Bayesian approach for x-ray and neutron scattering spectroscopy," in *Inelastic X-Ray Scattering and X-Ray Powder Diffraction Applications*, edited by A. Cunsolo, M. K. K. D. Franco, and F. Yokaichiya (IntechOpen, 2020), Chap. 2, p. 26.

[26] A. De Francesco, F. Formisano, L. Scaccia, E. Guarini, U. Bafile, A. Alatas, S. T. Lynch, and A. Cunsolo, "Ice phonon spectra and Bayes inference: A gateway to a new understanding of terahertz sound propagation in water," J. Chem. Phys. **158**, 134509 (2023).

[27] A. De Francesco, L. Scaccia, F. Formisano, E. Guarini, U. Bafile, D. Nykypanchuk, A. Alatas, M. Li, S. T. Lynch, and A. Cunsolo, "The effect of embedded nanoparticles on the phonon spectrum of ice: An inelastic x-ray scattering study," Nanomaterials **13**, 918 (2023).

[28] A. De Francesco, L. Scaccia, R. B. Lennox, E. Guarini, U. Bafile, P. Falus, and M. Maccarini, "Model-free description of polymer-coated gold nanoparticle dynamics in aqueous solutions obtained by Bayesian analysis of neutron spin echo data," Phys. Rev. E **99**, 052504 (2019).

[29] W. R. Gilks, S. Richardson, and D. J. Spiegelhalter, *Markov Chain Monte Carlo in Practice* (Chapman & Hall/CRC, 1996).

[30] L. Tierney, "Markov chains for exploring posterior distributions," Ann. Stat. **22**, 1701–1762 (1994).

[31] P. J. Green, "Reversible jump Markov chain Monte Carlo computation and Bayesian model determination," Biometrika **82**, 711–732 (1995).

[32]U. Bafile, E. Guarini, and F. Barocchi, "Collective acoustic modes as renormalized damped oscillators: Unified description of neutron and x-ray scattering data from classical fluids," Phys. Rev. E **73**, 061203 (2006).
[33]F. Barocchi, U. Bafile, and M. Sampoli, "Exact exponential function solution of the generalized Langevin equation for autocorrelation functions of many-body systems," Phys. Rev. E **85**, 022102 (2012).
[34]F. Barocchi and U. Bafile, "Expansion in Lorentzian functions of spectra of quantum autocorrelations," Phys. Rev. E **87**, 062133 (2013).
[35]F. Barocchi, E. Guarini, and U. Bafile, "Exponential series expansion for correlation functions of many-body systems," Phys. Rev. E **90**, 032106 (2014).
[36]J. P. Hansen and I. R. McDonald, *Theory of Simple Liquids* (Academic Press, London, 1986).
[37]E. Guarini, S. Bellissima, U. Bafile, E. Farhi, A. De Francesco, F. Formisano, and F. Barocchi, "Density of states from mode expansion of the self-dynamic structure factor of a liquid metal," Phys. Rev. E **95**, 012141 (2017).
[38]S. Bellissima, M. Neumann, E. Guarini, U. Bafile, and F. Barocchi, "Density of states and dynamical crossover in a dense fluid revealed by exponential mode analysis of the velocity autocorrelation function," Phys. Rev. E **95**, 012108 (2017).
[39]E. Guarini, A. De Francesco, U. Bafile, A. Laloni, B. G. del Rio, D. J. Gonzalez, L. E. Gonzalez, F. Barocchi, and F. Formisano, "Neutron Brillouin scattering and *ab initio* simulation study of the collective dynamics of liquid silver," Phys. Rev. B **102**, 054210 (2020).
[40]E. Guarini, F. Barocchi, A. De Francesco, F. Formisano, A. Laloni, U. Bafile, M. Celli, D. Colognesi, R. Magli, A. Cunsolo, and M. Neumann, "Collective dynamics of liquid deuterium: Neutron scattering and approximate quantum simulation methods," Phys. Rev. B **104**, 174204 (2021).
[41]A. Cunsolo, "The THz spectrum of density fluctuations of water: The viscoelastic regime," Adv. Condens. Matter Phys. **2015**, 137435.
[42]H. E. Fischer, F. J. Bermejo, G. J. Cuello, M. T. Fernández-Díaz, J. Dawidowski, M. A. González, H. Schober, and M. Jimenez-Ruiz, "Quantitative evaluation of anharmonic and disorder effects on glassy dynamics," Phys. Rev. Lett. **82**, 1193–1196 (1999).
[43]A. Cunsolo, A. Suvorov, and Y. Q. Cai, "The onset of shear modes in the high frequency spectrum of simple disordered systems: Current knowledge and perspectives," Philos. Mag. **96**, 732–742 (2016).
[44]L. del Rosso, M. Celli, D. Colognesi, S. Rudić, N. English, and L. Ulivi, "Density of phonon states in cubic ice Ic," J. Phys. Chem. C **125**, 23533–23538 (2021).
[45]L. Van Hove, "The occurrence of singularities in the elastic frequency distribution of a crystal," Phys. Rev. **89**, 1189–1193 (1953).